Cellular/Molecular

Functional Control of Cold- and Menthol-Sensitive TRPM8 Ion Channels by Phosphatidylinositol 4,5-Bisphosphate

Beiying Liu and Feng Qin

Department of Physiology and Biophysical Sciences, State University of New York at Buffalo, Buffalo, New York 14214

Cold is detected by a small subpopulation of peripheral thermoreceptors. TRPM8, a cloned menthol- and cold-sensitive ion channel, has been suggested to mediate cold transduction in the innocuous range. The channel shows a robust response in whole-cell recordings but exhibits markedly reduced activity in excised membrane patches. Here we report that phosphatidylinositol 4,5-bisphosphate (PIP_2) is an essential regulator of the channel function. The rundown of the channel is prevented by lipid phosphatase inhibitors. Application of exogenous PIP_2 both activates the channel directly and restores rundown activity. Whole-cell experiments involving intracellular dialysis with polyvalent cations, inhibition of PIP_2 synthesis kinases, and receptor-mediated hydrolysis of PIP_2 show that PIP_2 also modulates the channel activity in the intact cells. The crucial role of PIP_2 on the function of TRPM8 suggests that the membrane PIP_2 level may be an important regulator of cold transduction *in vivo*. The opposite effects of PIP_2 on the vanilloid receptor TRPV1 and TRPM8 also implies that the membrane lipid may have dual actions as a bimodal switch to selectively control the heat- and cold-induced responses in nociceptors expressing both channels.

Key words: cold; menthol; temperature; pain; TRP channels; sensory neurons

Introduction

Cold sensation is elicited when the skin is cooled to temperatures below the thermoneutral zone (31–36°C). Several cold-sensitive ion channels have recently been identified (Maingret et al., 2000; Askwith et al., 2001; McKemy et al., 2002; Peier et al., 2002; Story et al., 2003). Among them, TRPM8 has been proposed for detection of cold temperatures in the innocuous range (McKemy et al., 2002; Peier et al., 2002). The receptor is present in both dorsal root ganglia (DRG) and trigeminal ganglia (TG) neurons of small diameters (probably Aδ and C fibers) (McKemy et al., 2002; Peier et al., 2002). Single-cell reverse transcription-PCR in combination with functional imaging suggests that the receptor is preferentially expressed within a subset of rapidly responsive, low-threshold, cold-sensitive neurons (Nealen et al., 2003; Thut et al., 2003). When expressed heterologously, TRPM8 shows properties reminiscent of those observed in cold- and menthol-sensitive neurons under similar conditions. The receptor is activated by menthol and by cooling temperatures <25–28°C. When both stimuli are applied together, menthol shifts the activation threshold of TRPM8 to warmer temperatures, consistent with the observation from the cold-responsive TG fibers (Hensel and Zoterman, 1951). TRPM8 is also robustly activated by icilin, a synthetic cooling compound, and by eucalyptol, the naturally occurring *Eucalyptus* derivative (McKemy et al., 2002). The activation by

icilin, cold, and menthol appears to involve different mechanisms (Andersson et al., 2004). The temperatures that activate TRPM8 are similar to those that activate the innocuous cold receptors *in vivo*.

The functional mechanisms of TRPM8 regulation and activation are mostly unknown. Cold and menthol appear to activate the channel via a membrane-delimited mechanism; however, pronounced differences are observed in excised patches and in intact neurons (Reid and Flonta, 2002; Voets et al., 2004). In particular, channels in excised patches show a strikingly low open probability, suggesting that the function of the receptor depends on the cellular environment. Here we address possible mechanisms underlying this apparent rundown of channel activity and attempt to identify appropriate conditions to prevent it. Intrigued by the effect of phosphatidylinositol 4,5-bisphosphate (PIP_2) on the rundown of other ion channels and transporters (Hilgemann and Ball, 1996; Hilgemann, 1997; Huang et al., 1998; Kobrinsky et al., 2000; Chuang et al., 2001; Hilgemann et al., 2001; Runnels et al., 2002), we examined its role on TRPM8. We find that fluoride-vanadate-pyrophosphate (FVPP), a mixture solution of phosphatase inhibitors (Friedman, 1993; Friedman, 1994; Huang et al., 1998; Liou et al., 1999), can stabilize channel currents in excised patches. Application of PIP_2 both activates the channel directly in the absence of stimuli and restores rundown responses to exogenous agonists. At the whole-cell level, dialysis of cells with polyvalent cations, inhibition of PIP_2 synthesis kinases, and hydrolysis of PIP_2 through activation of phospholipase C (PLC)-coupled surface receptors all led to inhibition of menthol and cold responses of the channel. From these results, we suggest that PIP_2 is essential to maintaining the function of the menthol and cold receptor ion channel TRPM8.

Materials and Methods

Materials. Purified brain phosphatidylinositol 4,5-bisphosphate was obtained from Calbiochem (La Jolla, CA) and Avanti. Purified brain phosphatidylinositol 4-phosphate was from Avanti (Alabaster, AL). The anti-PIP$_2$ antibody was from Assay Designs (Ann Arbor, MI). 1-Oleoyl-2-acetyl-sn-glycerol (OAG) was from Calbiochem. All other chemicals, including menthol, wortmannin, phenylarsine oxide (PAO), nerve growth factor (NGF), bisindolylmaleimide I (BIM), calphostin C, thapsigargin, isonitol-1,4,5-triphosphate (IP$_3$) poly-L-lysine (PLL; molecular weight, >300,000), ruthenium red, spermine, and carbachol, were from Sigma (St. Louis, MO).

Water-insoluble reagents were dissolved in either 100% ethanol or DMSO to make a stock solution and were diluted into recording solution at the appropriate concentration before the experiment. The final concentrations of ethanol and DMSO did not exceed 0.17 and 0.3%, respectively. PIP$_2$ was diluted in distilled water (1 mg/ml) and sonicated for ~15 min to form liposomes (20–200 nm) before application. Drug delivery was controlled by a gravity-driven local perfusion system (ALA Scientific Instruments) or intracellular dialysis through a patch pipette for 5–10 min after membrane breakthrough. The recording apparatus and perfusion lines were always thoroughly washed with ethanol after experiments.

Heterologous expression. Rat TRPM8 from trigeminal ganglions cloned in a pFROG vector was kindly provided by David Julius (University of California, San Francisco, San Francisco, CA) (McKemy et al., 2002). cDNAs for trkA (wild-type and mutants) and p75, which originated from David Julius (Prescott and Julius, 2003), were obtained from Jan Yang (Columbus University, Picayune, MS) (Wu et al., 2002), and the plasmid containing the rat muscarinic type 1 (M$_1$) receptor was provided by Jan Feng and Zeng Yan (State University of New York at Buffalo). For RNA preparation, rat TRPM8 in pFROG vector was linearized by *MluI* digest. Capped cRNAs were transcribed *in vitro* using the mMessage mMachine kit (Ambion Inc.). The final cRNA was resuspended in RNase-free water to ~1 ng/nl and kept at −80°C.

Human embryonic kidney 293 (HEK293) cells were maintained in DMEM plus 10% fetal bovine serum (HyClone, Logan, UT) with 1% penicillin and streptomycin, incubated at 37°C in 5% CO$_2$, and transfected at a confluence of ~80% using the standard calcium phosphate precipitation method. Either green fluorescent protein or human CD8 lymphocyte antigen (0.5 μg/0.2 ml) was cotransfected as a surface marker (Jurman et al., 1994). Electrophysiological recordings took place 10–28 h after transfection. For cells cotransfected with CD8, antibody-coated beads were used to visually identify the transfected cells (Dynabeads M450 CD8; Dynal, Lake Success, NY). More than 90% of the bead-marked cells appeared to express the channel.

Xenopus oocytes are used mostly for single-channel and macropatch recordings. *Xenopus laevis* oocytes were surgically removed, enzymatically separated using collagenase, and hand-selected 1 or 2 d after harvesting for microinjection of the channel cRNA. Typically, each oocyte received 10–30 ng of cRNA. The injected oocytes were incubated in ND96 (in mM: 96 NaCl, 1 MgCl$_2$, 2 KCl, 5 HEPES, 1.8 CaCl$_2$, pH 7.4) solution supplemented with 2.5 mM sodium pyruvate, 100 U/ml penicillin, and 100 μg/ml streptomycin at 18°C for 2–7 d before use.

Electrophysiology. Conventional whole-cell and excised patch-clamp recording methods were used. Currents were amplified using either an Axopatch 200B (Axon Instruments, Foster City, CA) or EPC-7 (Warner Instruments) patch-clamp amplifier, filtered at 1 kHz, and digitized at 5 kHz directly onto the computer hard disk through a BNC-2090/MIO acquisition system (National Instruments, Austin, TX) driven by custom-designed software (QuB/IcE). Patch electrodes were fabricated from borosilicate glass (Sutter Instrument, Novato, CA). Thin-wall capillaries were used for macropatch pipettes. All experiments except those on cold activation were conducted at room temperature (22–24°C).

The control bath solution for HEK293 cells was composed of (in mM): 140 NaCl, 5 KCl, 10 HEPES, and 30 glucose, pH 7.4 (adjusted with NaOH). The solution was supplemented with 1.8 mM Ca^{2+} for the Ca^{2+}-containing solution or 1–5 mM EGTA for the Ca^{2+}-free solution. FVPP solution, which chelated Mg^{2+}, also contained (in mM): 5 NaF, 0.1

Na$_3$VO$_4$, and 20 Na$_3$HP$_2$O$_7$. The pipette solution consisted of (in mM): 140 CsCl and 10 HEPES, pH 7.4 (adjusted with CsOH). The bath and pipette solutions for excised patch recordings in oocytes were symmetrical and contained 100 mM Na gluconate and 10 mM NaCl instead of 140 mM NaCl, and other components were the same as in the Ca^{2+}-free bath solution for HEK293 cells.

Temperature control. Cells were placed in a narrow, rectangular chamber. The temperature was controlled by exchanging the entire content of the recording bath through an inline SH-27B heater powered by a TC-324B temperature controller (Warner Instruments). The actual temperature of the recording was monitored using a miniature thermocouple (Warner Instruments) placed ~1 mm from the pipette tip. The temperature drop between the tip and the thermocouple was <0.5°C (Liu et al., 2003). The reported temperatures corresponded to the readout of the thermocouple without corrections.

Results

Spontaneous rundown of TRPM8 currents is prevented by FVPP

TRPM8 exhibits strong responses to menthol and/or cold in either whole-cell (broken patch) or cell-attached recordings, but the currents run down in a cell-free configuration. Figure 1A shows a representative recording from a *Xenopus* oocyte macropatch. The pipette solution contained 100 μM menthol. The patch was initially maintained in the cell-attached mode, in which application of a holding potential at −60 mV induced a large, sustained current. The patch was then excised into the normal bath solution in the inside-out configuration. The excision caused a progressive loss of channel activity. The rundown is generally fast and follows an exponential decay with a half-decay time of $t_{1/2} = $ ~11 s ($n = 5$) (Fig. 1C). The rundown is also relatively complete, resulting in a loss of ~90% of the on-cell activity. Single-channel recordings indicate that the unitary current amplitudes of the channel do not change during rundown (data not shown), suggesting that the rundown involves a decrease in either the open probability or the number of active channels or both.

The rundown of some ion channels is ascribed to protein or lipid dephosphorylation, which may be induced or enhanced by Mg^{2+} and inhibited by FVPP solution, a mixture of phosphatase inhibitors (Huang et al., 1998). We examined whether Mg^{2+} and FVPP alter the rundown properties of TRPM8. As shown in Figure 1B, inclusion of 1.8 mM Mg^{2+} in the bath solution significantly accelerates the rundown time course, resulting in a nearly fourfold increase on the half-decay rate (Fig. 1C). FVPP, on the other hand, prevents the rundown of the currents for the most part. Although there is a decrease in the current immediately after the patch excision, the reduction is generally small (Fig. 1C). Furthermore, after the initial decay, the response appeared to stabilize at a steady-state level. This is contrary to channels in the presence of Mg^{2+} or the normal bath solution, in which the rundown is nearly complete. The effect of Mg^{2+} is irreversible. Once rundown occurred, the exposure of the patch to the Mg^{2+}-free solution with or without FVPP failed to recover the channel activity.

Cold-activated currents of TRPM8 exhibit a rundown similar to that seen with menthol-activated currents on many aspects, including the acceleration by cytosolic Mg^{2+} and the prevention by FVPP (Fig. 1D,E). However, the rundown of cold responses shows two distinct features. First, the rundown is biphasic. Immediately after patch excision, a transient increase of the current was observed in all patches (Fig. 1D). The recursion was substantial in size, with an averaged amplitude of approximately half the initial cell-attached current. The time course of the recursion was

also fast, with a half-maximal time of $t_{1/2} =$ ~1 ± 0.2 s ($n = 5$). Such a large overshoot of response on patch excision was not observed in menthol-activated currents at room temperature, suggesting that its occurrence is cold-specific. Second, the rundown of the cold response in the normal bath solution became markedly slower than that of the menthol current. The half-decay time was estimated to be ~98 sec at 10°C (Fig. 1F). This is ~10-fold as slow as the rundown of the menthol activity at room temperature, suggesting that the underlying mechanism of the rundown is highly temperature-dependent [temperature coefficient (Q_{10}) = ~9]. In the presence of Mg^{2+}, however, the rundown of menthol and cold responses showed a similar time course ($t_{1/2} = 3 ± 0.3$ s; $n = 4$; vs $2 ± 0.75$ s; $n = 5$).

PIP$_2$ restores channel activity

The dependence of the rundown of TRPM8 on Mg^{2+} and FVPP is reminiscent of that of inwardly rectifying K$^+$ channels, for which PIP$_2$ has been implicated as a primary determinant (Huang et al., 1998). To assess whether PIP$_2$ has a similar role on TRPM8, we first examined the effect of a PIP$_2$-specific antibody on the function of the channel. Figure 2A illustrates a recording from a *Xenopus* oocyte patch in the FVPP bath solution. As before, with 100 μM menthol included in the pipette solution, a large current was evoked at −60 mV in the cell-attached mode. The current sustained after excision of the patch into the inside-out configuration. In the presence of FVPP, however, the addition of the PIP$_2$ antibody (28.5 μg/ml) to the patch resulted in nearly full inhibition of the current, as if the channel ran down. A similar inhibitory effect was observed in all patches ($n = 6$). To further support the function of PIP$_2$, we tested whether exogenous PIP$_2$ restores channel activity after rundown. Figure 2B shows an exemplar recording obtained under conditions similar to those in the previous experiments, except that the normal bath solution was used instead. The rundown of the channel activity was induced by excision of the patch into the bath solution, followed by perfusion with the Mg^{2+}-containing solution. Subsequent application of 20 μM exogenous PIP$_2$ to the cytosolic side of the patch reactivated a substantial current. The current evolved slowly, with $t_{1/2} = $ ~50 s (Fig. 2D). The recovery was incomplete in most patches, but on average it reached ~76% of the activity before patch excision (Fig. 2D). The restored activity was also inhibited by Mg^{2+}, as was the original current.

In addition to recovery of rundown activity, PIP$_2$ activates TRPM8 directly in the absence of external stimuli. Figure 2C shows a recording from an excised oocyte membrane patch superperfused with 20 μM PIP$_2$. Before application of PIP$_2$, the patch was exposed to the Mg^{2+}-containing solution after patch excision. The current evoked by PIP$_2$ was also developed slowly and had a time course similar to that of PIP$_2$-induced recovery of
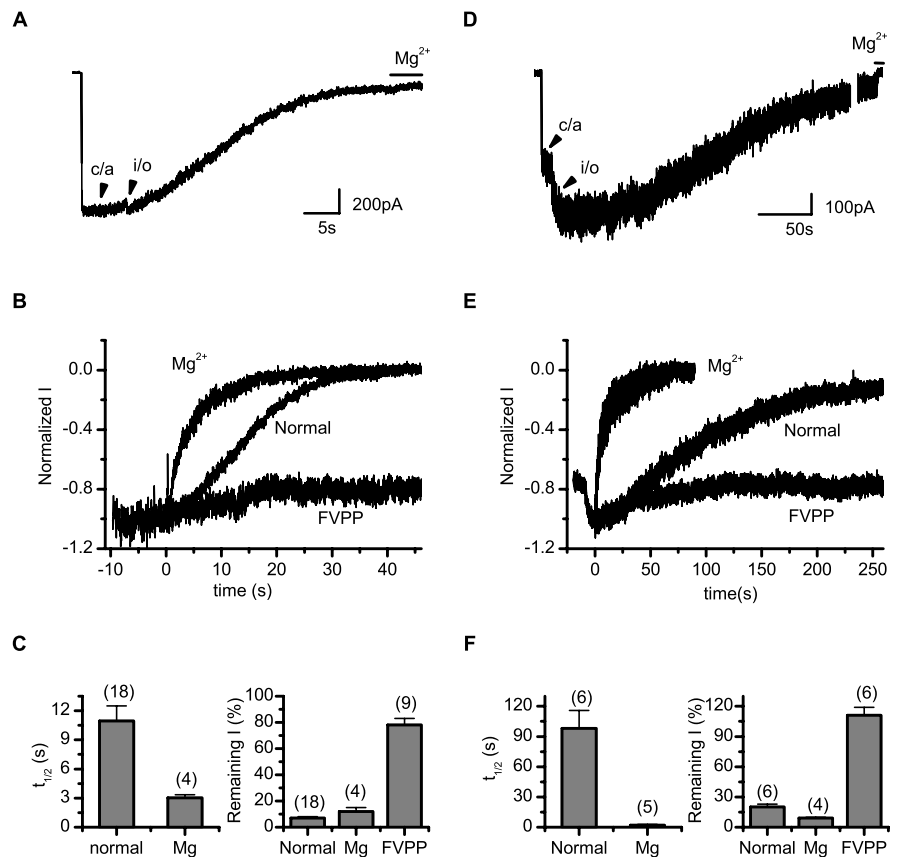

Figure 1. Rundown of TRPM8 channels. *A*, Representative trace for the rundown of currents recorded from a *Xenopus* oocyte membrane patch. The patch was initially maintained in the cell-attached (c/a) mode and then excised into the normal bath solution. The pipette solution contained 100 μM menthol. Mg^{2+} (1.8 mM) was applied at the end to examine the extent of rundown. Currents were evoked with $V_h = -60$ mV at room temperature (~22°C). *B*, Comparison of the time course of rundown in the normal bath solution and solutions containing Mg^{2+} and FVPP, respectively. The currents were normalized with the on-cell responses as the maximum and the residual currents after exposure to Mg^{2+} as the minimum. *C*, Quantification of the rundown under different conditions. The rundown rate was measured as the half-decay time relative to the initial cell-attached responses. *D–F*, Parallel experiments for cold responses at 10°C. i/o, Inside-out.

menthol responses ($t_{1/2} = 55 ± 15$ s; $n = 5$) (Fig. 2D). It eventually reached a considerable amplitude in the steady state (551 ± 76 pA; $n = 5$), which was approximately half the restored current in the presence of 100 μM menthol. The fact that PIP$_2$ activated a much smaller current in the absence of menthol than in the presence of menthol indicates that the activity in the latter case was not merely an effect of PIP$_2$ but indeed involved restoration of the menthol responses.

To gain some insights into the mechanisms of the actions of PIP2, we examined its effects on the sensitivity of TRPM8 to menthol. Figure 2E shows the concentration dependence of menthol responses under the condition with or without the inclusion of 30 μM PIP$_2$ in the pipette solution. The currents were recorded from isolated membrane patches in the outside-out configuration with FVPP included in both bath and pipette to prevent channel rundown. The dose–response curves were fit with the Hill equation, giving EC$_{50}$ = 36 μM and $n = 1.3$ in the absence of PIP$_2$ and EC$_{50}$ = 12 μM and $n = 1.1$ in the presence of PIP$_2$. The addition of PIP$_2$ therefore resulted in a leftward shift of the dose–response curve to menthol, suggesting that the effect of PIP$_2$ is not simply mediated by recruitment of silent channels but rather involves an allosteric interaction that alters sensitivity
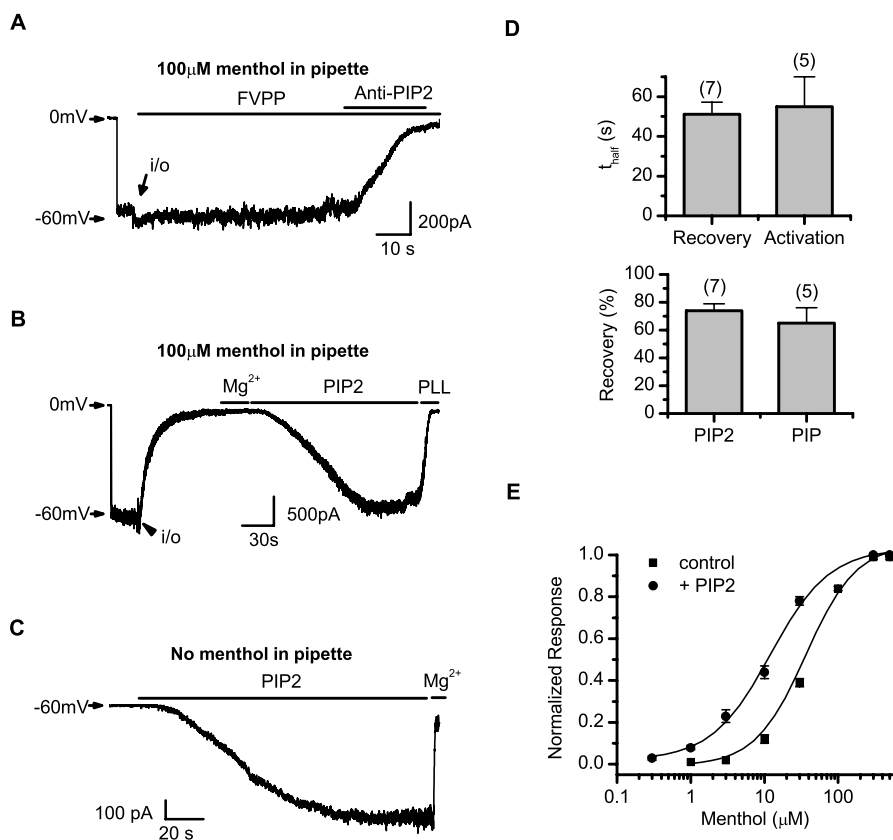
Figure 2. Effects of PIP2 on TRPM8 in excised patches. **A**, A monoclonal antibody (28.5 μg/ml) specific to PIP$_2$ inhibited channel activity. The recording was made in the FVPP bath solution with 100 μM menthol included in the pipette. **B**, Application of PIP$_2$ (20 μM) restored channel activity after rundown. The normal bath solution was used, and other conditions were the same as in **A**. PIP$_2$ was delivered to the cytoplasmic face in the FVPP solution. **C**, Direct activation of the channel by PIP$_2$ (20 μM). Before application of PIP$_2$, the patch was first excised into the normal bath solution to allow for rundown of a small spontaneous activity and then further exposed to the Mg^{2+}-containing solution for a complete rundown. **D**, Half-maximal times of PIP$_2$-induced recovery and activation and the steady-state amplitudes of the currents restored by PIP$_2$ and PIP expressed as a percentage of the currents obtained before patch excision. **E**, Dose–response curves of menthol-activated currents recorded under the condition with and without the inclusion of 30 μM PIP$_2$ in the pipette solution. FVPP was present in both bath and pipette to prevent channel rundown. The solid lines represent fits to the Hill equation, with EC$_{50}$ = 36 μM and n = 1.3 in the absence of PIP$_2$ (4–10 patches) and EC$_{50}$ = 12 μM and n = 1.1 in the presence of PIP$_2$ (4–12 patches). All recordings were from *Xenopus* oocyte membrane patches with the inside-out (i/o) configuration for **A–D** and the outside-out configuration for **E**. Holding potential, −60 mV.

to other stimuli. We also investigated the specificity of PIP$_2$ in restoring the rundown channel. Similar to the experiment with PIP$_2$ shown in Figure 2B, application of 20 μM PI(4)P restored channel activity after rundown. The average recovery, measured as the amplitude of the restored current relative to the initial response before patch excision, was estimated to be ~65% (n = 5) (Fig. 2D, bottom graph), which was close to that of PIP$_2$ (74%; n = 7). The data suggest that the effect of PIP$_2$ is not highly specific.

Polyvalent cations inhibit TRPM8
We next investigated whether PIP$_2$ modulates TRPM8 in the intact cells. Our first set of experiments examined whether polyvalent cations, which often act as a PIP$_2$ scavenger, inhibit TRPM8 activity. Figure 3A shows examples of recordings from an HEK293 cell transiently expressing TRPM8. The cell was internally dialyzed with 0.01% PLL. The activity of the channel was monitored by intermittent perfusion with 100 μM menthol over a total period of 10–15 min. The inhibition was quantified by the reduction of the current remaining after ~10 min dialysis relative to the current immediately after the patch break-in. As shown in

Figure 3B, the dialysis of cells with PLL caused a significant reduction (~90%) in menthol-evoked currents. The inhibition was apparently not attributable to dilution of regulatory molecules into the pipette solution or internalization of channel proteins. Control experiments with the normal pipette solution showed little change in currents over a similar period (Fig. 3B). We also examined other polyvalent cations, including ruthenium red (RR) and spermine. RR, which blocks TRPV1 by direct binding to the outer segment of the channel, inhibited TRPM8 by ~80% at 20 μM (Fig. 3B). Spermine was less effective, giving rise to ~60% of inhibition at 50 μM.

Parallel experiments were performed on cold activity of TRPM8. Figure 3C illustrates the whole-cell currents from transiently transfected HEK293 cells in response to cooling (10°C). Both RR and spermine inhibited the channel activity, although the effects appeared less profound than on menthol responses at room temperature (Fig. 3D). Together, these results suggest that the polyvalent cations have a strong inhibitory role on the function of TRPM8, which is consistent with the notion that they could sequester PIP$_2$ and therefore prevent it from interacting with the channel.

Blocking PIP$_2$ synthesis inhibits channel activity
The phosphoinositide (PI) 4-kinases are involved in synthesis of PIP$_2$ in the plasma membrane (Nakanishi et al., 1995; Meyers and Cantley, 1997; Varnai and Balla, 1998). Inhibition of the kinases has been reported to prevent replenishment of PIP$_2$ in a variety of cells, and a long-term treatment will deplete PIP$_2$ from unstimulated cells, presumably because of ongoing endogenous hydrolysis of PIP$_2$ (Wiedemann et al., 1996; Willars et al., 1998; Suh and Hille, 2002). We examined whether blockers of the PI 4-kinases such as wortmannin inhibits TRPM8. As shown in Figure 4A, the inclusion of 10 μM wortmannin in the pipette solution caused a progressive decay on the whole-cell currents evoked by 100 μM menthol in transiently transfected HEK293 cells. On average, the reduction of the currents was >80% after ~10 min of treatment (Fig. 4B). Because a high concentration of wortmannin blocks both PI 3- and PI 4-kinases, we repeated the experiment with 1 μM wortmannin, a concentration that is known to inhibit PI 3- but not PI 4-kinases. The effect of wortmannin at this concentration was considerably weaker, with an overall reduction of current of <15%. The data therefore suggest that the PI 4-kinases, not the PI 3-kinases, were primarily responsible for the inhibition of the channel observed at 10 μM wortmannin.

Wortmannin also inhibits the myosin light chain kinase (Okada et al., 1994; Nakanishi et al., 1995). To ensure the involvement of PI 4-kinases, we tested another chemically distinct inhibitor of the PI 4-kinase, PAO, which blocks the formation of PIP$_2$ from PI (Wiedemann et al., 1996; Sorensen et al., 1998; Varnai
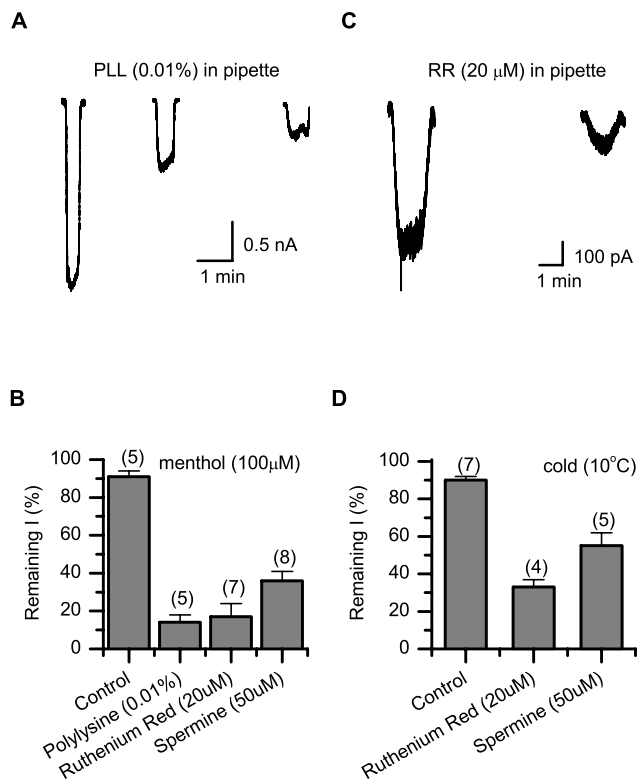
A

PLL (0.01%) in pipette

C

RR (20 μM) in pipette

0.5 nA
1 min

100 pA
1 min

B

menthol (100μM)

Remaining I (%)

Control / Polylysine (0.01%) / Ruthenium Red (20μM) / Spermine (50uM)

D

cold (10°C)

Remaining I (%)

Control / Ruthenium Red (20uM) / Spermine (50uM)

Figure 3. Inhibition of TRPM8 by polyvalent cations. **A**, Intracellular dialysis of PLL (0.01%) through a patch pipette inhibited whole-cell currents induced by 100 μM menthol in HEK293 cells. The first response was recorded immediately after break-in to the whole-cell configuration. **B**, Summary graph of the effects of different polyvalent cations. The inhibition was determined as the percentage of peak current remaining in an interval of ∼10 min relative to the initial response after patch break-in. **C, D**, Inhibition of cold-induced activity of the channel. Cooling was applied by exchanging the bath content with solutions precooled to 10°C, followed by warming back to room temperature. All recordings were made at a holding potential of −60 mV.

and Balla, 1998). As summarized in Figure 4*B*, PAO at 10 μM was more effective than wortmannin, producing an inhibition of >90% on menthol-activated currents.

The effects of wortmannin and PAO on cold-activated currents of TRPM8 were similar to those on menthol responses. Figure 4*C* shows whole-cell recordings from a TRPM8-expressing HEK293 cell in response to cooling from room temperature to 10°C. Both wortmannin and PAO at 10 μM significantly inhibited the channel (Fig. 4*D*). In contrast, wortmannin at 1 μM was much less effective, further supporting the involvement of PI 4-kinases rather than PI 3-kinases.

To ensure that the effects of wortmannin and PAO resulted from the inhibition of lipid kinases, we tested the inhibitors for their possible direct effects on the channel. Figure 4*E* illustrates a current recording from an excised outside-out patch applied with 100 μM menthol in the absence and presence of the inhibitors. Application of either 10 μM wortmannin or 10 μM PAO showed no significant effect on the response of 100 μM menthol (Fig. 4*F*). The data therefore suggest that the profound inhibition of menthol and cold responses in the whole-cell condition must arise from the inhibition of PIP_2 synthesis rather than a direct interaction of the compounds with the channel itself.

Receptor-mediated hydrolysis of PIP_2 inhibits TRPM8

To further understand the PIP_2 dependence of the channel, we studied the effects of receptor-mediated hydrolysis of PIP_2 on TRPM8 function. The channel was coexpressed in HEK293 cells
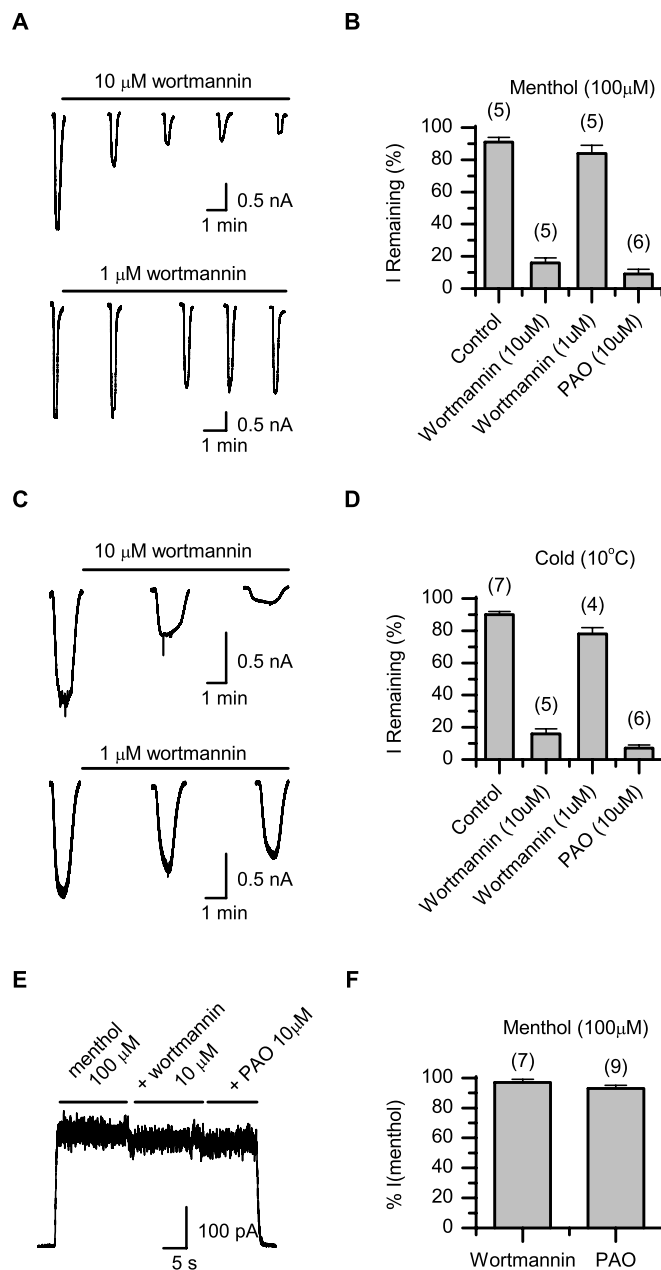
A

10 μM wortmannin

0.5 nA
1 min

1 μM wortmannin

0.5 nA
1 min

B

Menthol (100μM)

I Remaining (%)

Control / Wortmannin (10uM) / Wortmannin (1uM) / PAO (10uM)

C

10 μM wortmannin

0.5 nA
1 min

1 μM wortmannin

0.5 nA
1 min

D

Cold (10°C)

I Remaining (%)

Control / Wortmannin (10uM) / Wortmannin (1uM) / PAO (10uM)

E

menthol 100 μM / + wortmannin 10 μM / + PAO 10μM

100 pA
5 s

F

Menthol (100μM)

% I (menthol)

Wortmannin / PAO

Figure 4. Block of PIP_2 synthesis inhibits TRPM8 activity. **A**, Representative whole-cell recordings showing the effects of wortmannin at 10 and 1 μM, respectively. Currents were evoked by 100 μM menthol applied externally. Wortmannin was dialyzed into the cell through the pipette solution. **B**, Comparison of the inhibition induced by wortmannin at 10 and 1 μM and by PAO at 10 μM. The percentage of current remaining at the end of ∼10 min application of the blockers relative to the first response was plotted. PAO was applied by extracellular perfusion. **C, D**, Effects of wortmannin and PAO on temperature responses. Currents were activated by cooling bath to 10°C as described previously. **E**, Current trace from an outside-out patch elicited by 100 μM menthol in the absence and presence of wortmannin and PAO, showing no direct effects of the inhibitors on the channel. FVPP was included in both bath and pipette solutions to prevent channel rundown. **F**, Summary graph for experiments in **E** showing the percentage currents in the presence of the inhibitors relative to the currents obtained with 100 μM menthol alone. Data were recorded at −60 mV from HEK293 cells transiently expressing TRPM8.

with the NGF receptor trkA, which directly activates PLC-γ for hydrolysis of PIP_2. A protocol similar to that used in the PI 4-kinase inhibition experiments was used, in which NGF was applied to cells for ∼10 min while the channel activity was briefly sampled at different times to monitor its changes. Figure 5*A* shows representative recordings of whole-cell currents evoked by
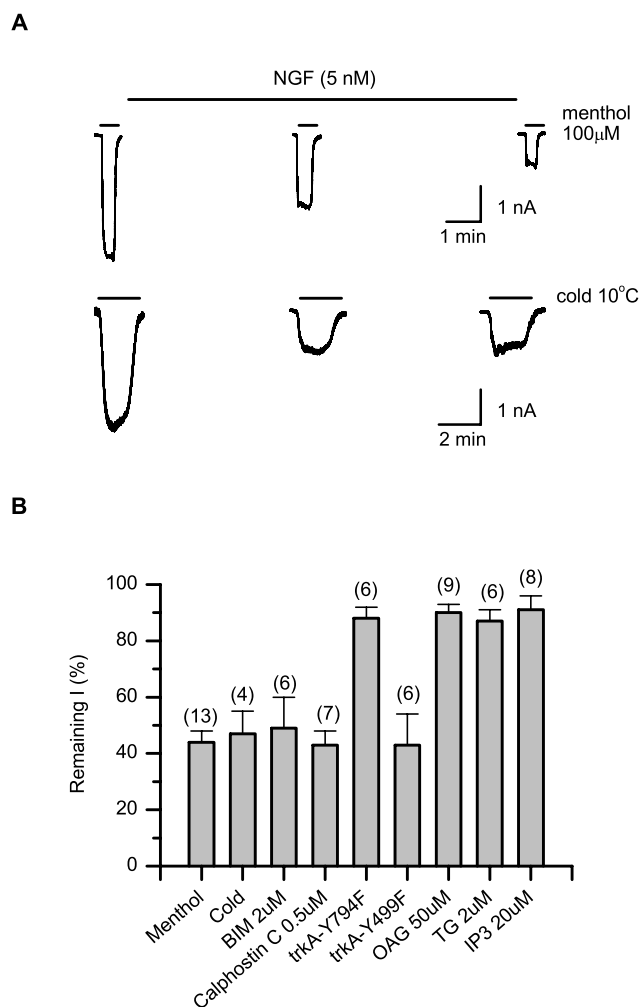
A

B

Figure 5. Inhibition of TRPM8 through trkA receptor-mediated hydrolysis of PIP$_2$. **A**, Whole-cell recordings on the effects of NGF on menthol and cold activity of the channel, respectively. NGF (5 nM) was applied externally for 10–20 min after the first recording. **B**, Summary graph of NGF-induced inhibition from different experiments including manipulation of each step in the signaling pathway downstream of the NGF receptor trkA. The NGF effect was evaluated as the percentage of remaining current after 10 min treatment relative to the initial response before treatment. Except explicitly noted, all experiments were performed with 100 μM menthol as the stimulus. Data were recorded at −60 mV from HEK293 cells transiently transfected with TRPM8 and the NGF receptor trkA/p75 or its mutants. TG, Thapsigargin.

menthol (100 μM) and temperature (10°C), respectively. Application of 5 nM NGF to cells expressing TRPM8 and trkA/p75 produced a partial but significant reduction in channel activity over a course of 5–10 min. The effects on menthol and cold responses were similar, with both currents reduced by ∼60% in 10 min relative to their initial responses immediately after whole-cell break-in (Fig. 5B). The partial inhibition of TRPM8 could be attributable to incomplete hydrolysis of PIP$_2$ because of the ongoing activity of PI 4-kinases. The inclusion of wortmannin in the pipette solution resulted in nearly complete inhibition (data not shown).

Stimulation of trkA receptors activates mitogen-activated protein kinase (MAPK) and PLC-γ (Stephens et al., 1994). The latter cleaves PIP$_2$ into two second messengers, diacylglycerol (DAG) and IP$_3$. The membrane-bound DAG recruits and activates protein kinase C (PKC), whereas IP$_3$ mobilizes calcium release from intracellular stores. To determine whether hydrolysis of PIP$_2$ is directly responsible for the NGF effect, we examined
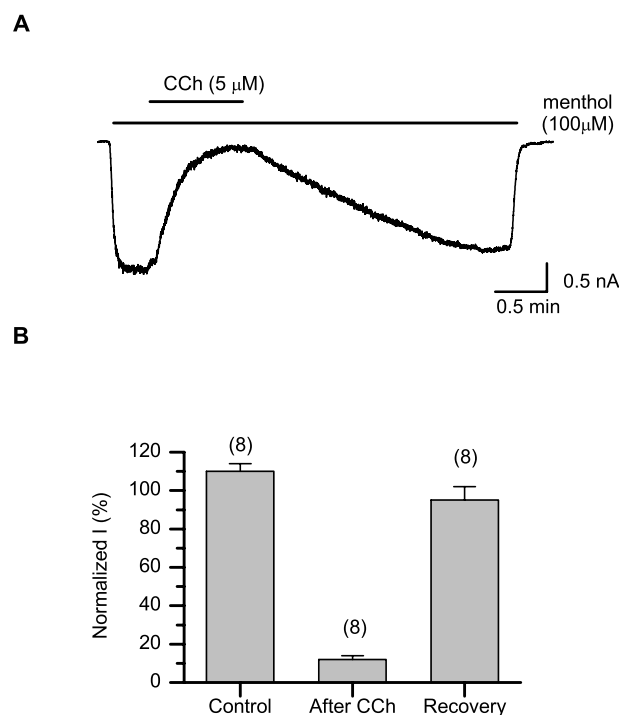
A

B

Figure 6. Inhibition of TRPM8 via muscarinic receptor-mediated hydrolysis of PIP$_2$. **A**, Whole-cell recording of menthol-activated currents from an HEK293 cell coexpressing TRPM8 and the rat M$_1$ receptor. Carbachol (CCh; 5 μM) was applied externally in the presence of menthol (100 μM). **B**, Summary plot of carbachol effects on TRPM8. The currents were normalized to the initial response of menthol before carbachol application. The control experiments corresponded to those with transfection of TRPM8 alone. All currents were elicited with 100 μM menthol at a holding potential of −60 mV.

each step in this signaling cascade. The involvement of the MAPK pathway was evaluated with two trkA mutants, Tyr499Phe and Tyr794Phe, which uncouple MAPK and PLC-γ from trkA, respectively (Stephens et al., 1994; Chuang et al., 2001; Prescott and Julius, 2003). As summarized in Figure 5B, activation of the Tyr499Phe mutant of trkA caused profound inhibition (57 $\pm$ 11%; $n = 6$) similar to that induced by the wild-type receptor on the whole-cell currents evoked by 100 μM menthol. In contrast, activation of the Tyr794Phe mutant had a much weaker effect (12 $\pm$ 4%; $n = 6$) under a similar condition. PLC-mediated hydrolysis of PIP$_2$ is therefore essential to the NGF effect. Downstream of PLC-γ, block of PKC by BIM at 2 μM or calphostin C at 0.5 μM produced no significant changes in NGF-induced inhibition. Similarly, either perfusion of cells with thapsigargin (2 μM) or intracellular dialysis with IP$_3$ (20 μM) did not inhibit the channel. The membrane-permeant DAG analog OAG had little effect at concentrations up to 50 μM, although some inhibition of activity was observed at 100 μM. Together, these results suggest that the NGF-induced inhibition of TRPM8 results directly from breakdown of PIP$_2$ rather than downstream signaling molecules and pathways.

To corroborate our results on the trkA receptor-mediated inhibition, we also examined whether G$_q$-protein-coupled receptors could confer similar effects on TRPM8. M$_1$ receptors activate PLC-β via G$_{\alpha q}$-containing heterotrimeric G-proteins (Peralta et al., 1988). Figure 6A illustrates a recording of whole-cell currents from an HEK293 cell transiently transfected with TRPM8 and the M$_1$ receptor. Stimulation of the M$_1$ receptor with 5 μM carbachol indeed profoundly suppressed the current elicited by 100 μM menthol. The inhibition was reversible because subsequent ap-

plication of menthol in the absence of carbachol mostly recovered the channel response. In contrast, cells that were not transfected with the M$_1$ receptor showed little effect of carbachol (50 μM) on menthol activity of TRPM8 (Fig. 6B). These results are in agreement with the transient decrease of the PIP$_2$ levels evoked by activation of G$_q$-coupled receptors and provide further evidence that the TRPM8 channel could be inhibited by surface receptor-mediated hydrolysis of PIP$_2$.

Discussion

In the present study, we show that the TRPM8 channel exhibits rapid rundown in excised membrane patches, and this process is accelerated by cytosolic application of Mg^{2+} and prevented by a mixture of general phosphatase inhibitors. Application of exogenous PIP$_2$ after channel rundown partially restored its responses to external stimuli, whereas PIP$_2$ alone activated the channel directly, albeit with a weaker response. Whole-cell experiments indicated that either intracellular dialysis with polyvalent cations or blockade of PI 4-kinases, which are involved in synthesis of PIP$_2$, resulted in significant inhibition of the channel activity. Finally, the receptor-mediated hydrolysis of PIP$_2$ also led to profound reduction of channel function in HEK293 cells expressing the TRPM8 and trkA/p75 receptors. Together, these data suggest that PIP$_2$ is a crucial element in maintaining the function of the TRPM8 channel.

The rundown of the cold-activated responses of TRPM8 showed some intriguing properties. First, the current exhibited a large transient increase before rundown. The excursion reached a magnitude of nearly half the cell-attached response and had a time course on the order of 1–2 s. This relatively fast time course of the overshoot may imply that the channel is persistently inhibited in intact cells by some diffusible cytosolic factors. However, such a large overshoot of current was not seen in the rundown of menthol-evoked responses at room temperatures, suggesting that a more complicated mechanism may be involved. Either the production of the inhibitor(s) was cold-sensitive, or the menthol activation of the channel is different from that by temperature.

The other surprising observation is that the rundown of the cold responses of the channel was nearly an order of magnitude slower than that of the menthol responses at room temperatures. The Q$_{10}$ of the rundown rate was ~9 as estimated from the half-decay time. This is unusually high even compared with the temperature coefficients of the gating of ion channels (Hille, 2001). The origin of this high temperature dependence is unclear. If the rundown of the channel is mediated by dephosphorylation of proteins or lipids, one possible implication is that the function of the necessary phosphatases is highly temperature-sensitive. Regardless of the underlying mechanisms, such a high Q$_{10}$ process will almost certainly have a positive impact on the temperature sensitivity of the channel itself.

The fact that PIP$_2$ both activates TRPM8 and is a prerequisite for exogenous stimuli appears paradoxical. If the binding of PIP$_2$ suffices to open the channel, what will menthol and temperature do? One possible explanation is that the channel interacts with multiple PIP$_2$ molecules, and the cell regulates the level of PIP$_2$ in the membrane so that it is insufficient to open the channel by itself but enough to enable activation by menthol or temperature. Studies of other ion channels suggest that the binding of PIP$_2$ tends to be electrostatic (Rohacs et al., 1999; Zhang et al., 1999; Prescott and Julius, 2003; Gambhir et al., 2004). Such an interaction has the virtue of flexibility to allow for multiple PIP$_2$ molecules interacting with the channel, thereby providing a potentially large number of degrees of freedom that can be tuned for

the strength of the interaction and the function of the channel. Whether PIP$_2$ modulates TRPM8 in a similar mechanism remains to be determined.

TRPM8 belongs to a superfamily of TRP ion channels. A recurring property of the members in this family is their regulation by membrane lipids. The founding members, the TRP, TRPL, and TRPγ ion channels, which are responsible for the PLC-mediated light response in *Drosophila melanogaster* (Montell and Rubin, 1989; Phillips et al., 1992), are suggested to require PIP$_2$ to maintain a sustained activity (Hardie et al., 2001). PIP$_2$ also reverses the desensitization of TRPM5 (Liu and Liman, 2003), and its hydrolysis leads to inactivation of the constitutive activity of the TRPM7 channel (Runnels et al., 2002). The lipid can also play an inhibitory role. TRPV1, another thermosensitive ion channel, is potentiated by displacement of PIP$_2$ from the channel (Chuang et al., 2001; Prescott and Julius, 2003). PIP$_2$ is not the only membrane lipid that modulates TRP channels. DAG, for example, has been shown to be a potent activator of mammalian TRPC3 and TRPC6 (Hofmann et al., 1999). It appears that membrane lipids, and PIP$_2$ in particular, have a widespread role on the regulation of the function of the TRP channels. The results presented here provide further evidence in support of the observation.

The effect of PIP$_2$ on TRPM8 raises questions about its physiological relevance in thermal sensation, especially under pathological conditions. Tissue injury and inflammation cause releases of proinflammatory hormones and messengers from local neurons and immune cells. Some ingredients of this inflammatory soup, e.g., NGF, may stimulate their signature surface receptors, leading to activation of PLC and subsequent hydrolysis of PIP$_2$ (Chuang et al., 2001). Although such a signaling transduction cascade has not been established in cold receptor cells, there is evidence indicating that trkA, an NGF receptor, and TRPM8 are coexpressed in these neurons (Peier et al., 2002). Given our finding on the profound effect of PIP$_2$ on TRPM8, it appears that the membrane lipid may also modulate the function of the channel *in vivo*, and the physiological sensation of cold could be altered under the inflammatory conditions. Recent studies of rat DRG neurons report that the presence of NGF in the culture medium increases the fraction of menthol-sensitive neurons and their sensitivity to temperature (Reid et al., 2002; Babes et al., 2004). Such results are not predicted by the acute inhibition of NGF-mediated PIP$_2$ hydrolysis on TRPM8, as observed in the heterologous expression systems. The differences therefore highlight the possible complexity of NGF actions on cold-sensitive neurons. It is conceivable that NGF may have both an inhibitory acute effect on the biophysical properties of the channel and a potentiatory long-term effect on gene expression or intracellular signaling. The latter may have caused the changes of the expression of cold-sensitive neurons and their temperature sensitivity in the NGF-treated culture.

It is intriguing that PIP$_2$ exerts opposite effects on TRPM8 and TRPV1. Although PIP$_2$ binding is required for the function of TRPM8, it inhibits the activity of TRPV1 (Chuang et al., 2001; Prescott and Julius, 2003). This raises the prospect that PIP$_2$ may have a more general role on the thermal sensation and pain transduction at the cellular level. For example, some studies have suggested that TRPM8 and TRPV1 are coexpressed in nociceptors (McKemy et al., 2002; Thut et al., 2003). The differential effects of PIP$_2$ on the two channels indicate that it could act as a bimodal switch to control the heat and cold sensitivity of these receptor cells. Future studies of native neurons may help elucidate the physiological effects of PIP$_2$ and possibly other membrane lipids on thermal transduction *in vivo*.

References

Andersson DA, Chase HW, Bevan S (2004) TRPM8 activation by menthol, icilin, and cold is differentially modulated by intracellular pH. J Neurosci 24:5364–5369.

Askwith CC, Benson CJ, Welsh MJ, Snyder PM (2001) DEG/ENaC ion channels involved in sensory transduction are modulated by cold temperature. Proc Natl Acad Sci USA 98:6459–6463.

Babes A, Zorzon D, Reid G (2004) Two populations of cold-sensitive neurons in rat dorsal root ganglia and their modulation by nerve growth factor. Eur J Neurosci 20:2276–2282.

Chuang HH, Prescott ED, Kong H, Shields S, Jordt SE, Basbaum AI, Chao MV, Julius D (2001) Bradykinin and nerve growth factor release the capsaicin receptor from PtdIns(4,5)P2-mediated inhibition. Nature 411:957–962.

Friedman ZY (1993) Tamoxifen and vanadate synergize in causing accumulation of polyphosphoinositides in GH4C1 membranes. J Pharmacol Exp Ther 267:617–623.

Friedman ZY (1994) The antitumor agent tamoxifen inhibits breakdown of polyphosphoinositides in GH4C1 cells. J Pharmacol Exp Ther 271:238–245.

Gambhir A, Hangyas-Mihalyne G, Zaitseva I, Cafiso DS, Wang J, Murray D, Pentyala SN, Smith SO, McLaughlin S (2004) Electrostatic sequestration of PIP2 on phospholipid membranes by basic/aromatic regions of proteins. Biophys J 86:2188–2207.

Hardie RC, Raghu P, Moore S, Juusola M, Baines RA, Sweeney ST (2001) Calcium influx via TRP channels is required to maintain PIP2 levels in *Drosophila* photoreceptors. Neuron 30:149–159.

Hensel H, Zotterman Y (1951) The effect of menthol on the thermoreceptors. Acta Physiol Scand 24:27–34.

Hilgemann DW (1997) Cytoplasmic ATP-dependent regulation of ion transporters and channels: mechanisms and messengers. Annu Rev Physiol 59:193–220.

Hilgemann DW, Ball R (1996) Regulation of cardiac Na+,Ca2+ exchange and KATP potassium channels by PIP2. Science 273:956–959.

Hilgemann DW, Feng S, Nasuhoglu C (2001) The complex and intriguing lives of PIP2 with ion channels and transporters. Sci STKE 2001:RE19, http://stke.sciencemag.org/cgi/content/full/oc_sigtrans; 2001/111/re19.

Hille B (2001) Ionic channels of excitable membranes. Sunderland, MA: Sinauer.

Hofmann T, Obukhov AG, Schaefer M, Harteneck C, Gudermann T, Schultz G (1999) Direct activation of human TRPC6 and TRPC3 channels by diacylglycerol. Nature 397:259–263.

Huang CL, Feng S, Hilgemann DW (1998) Direct activation of inward rectifier potassium channels by PIP2 and its stabilization by Gbetagamma. Nature 391:803–806.

Jurman ME, Boland LM, Liu Y, Yellen G (1994) Visual identification of individual transfected cells for electrophysiology using antibody-coated beads. Biotechniques 17:876–881.

Kobrinsky E, Mirshahi T, Zhang H, Jin T, Logothetis DE (2000) Receptor-mediated hydrolysis of plasma membrane messenger PIP2 leads to K+-current desensitization. Nat Cell Biol 2:507–514.

Liou HH, Zhou SS, Huang CL (1999) Regulation of ROMK1 channel by protein kinase A via a phosphatidylinositol 4,5-bisphosphate-dependent mechanism. Proc Natl Acad Sci USA 96:5820–5825.

Liu B, Hui K, Qin F (2003) Thermodynamics of heat activation of single capsaicin ion channels VR1. Biophys J 85:2988–3006.

Liu D, Liman ER (2003) Intracellular Ca2+ and the phospholipid PIP2 regulate the taste transduction ion channel TRPM5. Proc Natl Acad Sci USA 100:15160–15165.

Maingret F, Lauritzen I, Patel AJ, Heurteaux C, Reyes R, Lesage F, Lazdunski M, Honore E (2000) TREK-1 is a heat-activated background K(+) channel. EMBO J 19:2483–2491.

McKemy DD, Neuhausser WM, Julius D (2002) Identification of a cold receptor reveals a general role for TRP channels in thermosensation. Nature 416:52–58.

Meyers R, Cantley LC (1997) Cloning and characterization of a wortmannin-sensitive human phosphatidylinositol 4-kinase. J Biol Chem 272:4384–4390.

Montell C, Rubin GM (1989) Molecular characterization of the *Drosophila* trp locus: a putative integral membrane protein required for phototransduction. Neuron 2:1313–1323.

Nakanishi S, Catt KJ, Balla T (1995) A wortmannin-sensitive phosphatidylinositol 4-kinase that regulates hormone-sensitive pools of inositol phospholipids. Proc Natl Acad Sci USA 92:5317–5321.

Nealen ML, Gold MS, Thut PD, Caterina MJ (2003) TRPM8 mRNA is expressed in a subset of cold-responsive trigeminal neurons from rat. J Neurophysiol 90:515–520.

Okada T, Sakuma L, Fukui Y, Hazeki O, Ui M (1994) Blockage of chemotactic peptide-induced stimulation of neutrophils by wortmannin as a result of selective inhibition of phosphatidylinositol 3-kinase. J Biol Chem 269:3563–3567.

Peier AM, Moqrich A, Hergarden AC, Reeve AJ, Andersson DA, Story GM, Earley TJ, Dragoni I, McIntyre P, Bevan S, Patapoutian A (2002) A TRP channel that senses cold stimuli and menthol. Cell 108:705–715.

Peralta EG, Ashkenazi A, Winslow JW, Ramachandran J, Capon DJ (1988) Differential regulation of PI hydrolysis and adenylyl cyclase by muscarinic receptor subtypes. Nature 334:434–437.

Phillips AM, Bull A, Kelly LE (1992) Identification of a *Drosophila* gene encoding a calmodulin-binding protein with homology to the trp phototransduction gene. Neuron 8:631–642.

Prescott ED, Julius D (2003) A modular PIP2 binding site as a determinant of capsaicin receptor sensitivity. Science 300:1284–1288.

Reid G, Flonta ML (2002) Ion channels activated by cold and menthol in cultured rat dorsal root ganglion neurones. Neurosci Lett 324:164–168.

Reid G, Babes A, Pluteanu F (2002) A cold- and menthol-activated current in rat dorsal root ganglion neurones: properties and role in cold transduction. J Physiol (Lond) 545:595–614.

Rohacs T, Chen J, Prestwich GD, Logothetis DE (1999) Distinct specificities of inwardly rectifying K+ channels for phosphoinositides. J Biol Chem 274:36065–36072.

Runnels LW, Yue L, Clapham DE (2002) The TRPM7 channel is inactivated by PIP(2) hydrolysis. Nat Cell Biol 4:329–336.

Sorensen SD, Linseman DA, McEwen EL, Heacock AM, Fisher SK (1998) A role for a wortmannin-sensitive phosphatidylinositol-4-kinase in the endocytosis of muscarinic cholinergic receptors. Mol Pharmacol 53:827–836.

Stephens RM, Loeb DM, Copeland TD, Pawson T, Greene LA, Kaplan DR (1994) Trk receptors use redundant signal-transduction pathways involving Shc and Plc-gamma-1 to mediate Ngf responses. Neuron 12:691–705.

Story GM, Peier AM, Reeve AJ, Eid SR, Mosbacher J, Hricik TR, Earley TJ, Hergarden AC, Andersson DA, Hwang SW, McIntyre P, Jegla T, Bevan S, Patapoutian A (2003) ANKTM1, a TRP-like channel expressed in nociceptive neurons, is activated by cold temperatures. Cell 112:819–829.

Suh BC, Hille B (2002) Recovery from muscarinic modulation of M current channels requires phosphatidylinositol 4,5-bisphosphate synthesis. Neuron 35:507–520.

Thut PD, Wrigley D, Gold MS (2003) Cold transduction in rat trigeminal ganglia neurons in vitro. Neuroscience 119:1071–1083.

Varnai P, Balla T (1998) Visualization of phosphoinositides that bind pleckstrin homology domains: calcium- and agonist-induced dynamic changes and relationship to myo-[3H]inositol-labeled phosphoinositide pools. J Cell Biol 143:501–510.

Voets T, Droogmans G, Wissenbach U, Janssens A, Flockerzi V, Nilius B (2004) The principle of temperature-dependent gating in cold- and heat-sensitive TRP channels. Nature 430:748–754.

Wiedemann C, Schafer T, Burger MM (1996) Chromaffin granule-associated phosphatidylinositol 4-kinase activity is required for stimulated secretion. EMBO J 15:2094–2101.

Willars GB, Nahorski SR, Challiss RA (1998) Differential regulation of muscarinic acetylcholine receptor-sensitive polyphosphoinositide pools and consequences for signaling in human neuroblastoma cells. J Biol Chem 273:5037–5046.

Wu L, Bauer CS, Zhen XG, Xie C, Yang J (2002) Dual regulation of voltage-gated calcium channels by PtdIns(4,5)P-2. Nature 419:947–952.

Zhang H, He C, Yan X, Mirshahi T, Logothetis DE (1999) Activation of inwardly rectifying K+ channels by distinct PtdIns(4,5)P2 interactions. Nat Cell Biol 1:183–188.